

# Nuclear actin polymerization from faster growing ends in the initial activation of hox gene transcription

## Are nuclear speckles involved?

Gabriela Naum-Onganía<sup>1,\*</sup>, Víctor M Díaz<sup>2</sup>, Francesco Blasi<sup>3</sup> and Rolando Rivera-Pomar<sup>1</sup>

<sup>1</sup>Centro Regional de Estudios Genómicos (CREG); Universidad Nacional de La Plata; Buenos Aires, Argentina; <sup>2</sup>Institut Municipal d'Investigació Mèdica (IMIM); Hospital del Mar; Barcelona, Spain; <sup>3</sup>Istituto FIRC di Oncologia Molecolare (IFOM); Milan, Italy; <sup>4</sup>Centro de Bioinvestigaciones; Universidad Nacional del Noroeste de Buenos Aires; Pergamino, Buenos Aires, Argentina

**Keywords:** nuclear actin, nuclear speckles, co-transcriptional splicing, RNA pol II, transcription/splicing, Hox genes

The *HoxB* cluster expression is activated by retinoic acid and transcribed in a collinear manner. The DNA-binding Pknox1-Pbx1 complex modulates Hox protein activity. Here, NT2-D1 teratocarcinoma cells—a model of *Hox* gene expression—were used to show that upon retinoic acid induction, Pknox1 co-localizes with polymeric nuclear actin. We have found that globular actin aggregates, polymeric actin, the elongating RNA polymerase II and THOC match euchromatic regions corresponding to nuclear speckles. Moreover, RNA polymerase II, N-WASP, and transcription/splicing factors p54<sup>nrb</sup> and PSF were validated as Pknox1 interactors by tandem affinity purification. PSF pulled down with THOC and nuclear actin, both of which co-localize in nuclear speckles. Although latrunculin A slightly decreases the general level of *HoxB* gene expression, inhibition of nuclear actin polymerization by cytochalasin D blocks the expression of *HoxB* transcripts in a collinear manner. Thus, our results support the hypothesis that nuclear actin polymerization is involved in the activation of *HoxB* gene expression by means of nuclear speckles.

### Introduction

The eukaryotic nucleus is compartmentalized in chromatin domains, which are both permissive and restrictive of transcription.<sup>1,2</sup> This process occurs in specific, but poorly characterized, nuclear subregions or transcription factories, in which active genes are concentrated together with RNA polymerase II (RNAP II) and DNA- and RNA-binding factors.<sup>3</sup>

Active genes are often seen to move outside of their chromosome territories as they are transcribed.<sup>2,4</sup> In this sense, it has been suggested that DNA might be moved within the nucleus into transcription factories<sup>3,5</sup> and, once there, DNA promoters might bound to the RNAP II that is fixed at these foci.<sup>6</sup> Nevertheless, new evidence strongly demonstrated that RNAP II clusters form transiently, which refutes the idea that transcription factories are statically assembled nuclear substructures.<sup>7</sup> RNAP II molecules are in motion in living cells, even on very highly expressed genes and they are concentrated by a self-assembly process to transcription regions, rather than by attachment to a nuclear structure.<sup>8</sup> Along this line, other relevant structures as the nuclear speckles—active compartments attached to the nuclear matrix—are related to the process of transcription, RNA processing, and

splicing.<sup>9</sup> Moreover, it has been shown that active genes co-localize with nuclear speckles rather than transcription factories.<sup>9–11</sup>

The expression of the HOX cluster is coordinated.<sup>12</sup> *Hox* genes are co-regulated and expressed in the order of their location in the genome.<sup>13</sup> This mechanism, termed collinearity, has been demonstrated in many systems, including cell lines where collinear expression is promoted upon retinoic acid (RA) induction. The induction of *HoxB* expression by RA is accompanied by the movement of the cluster outside the chromosomal territory and toward the center of the nucleus. This process occurs in a temporal pattern that parallels that of gene expression from the locus. According to this line, it has been suggested that the localization outside the chromosomal territory may be a visual manifestation of chromatin decondensation.<sup>4,14</sup>

Among the regulators of *Hox* gene activity, Prep1, onwards called Pknox1 (Pbx knotted homeobox 1), is a homeodomain-containing factor<sup>15</sup> necessary for the expression of the proximal genes of the cluster (early genes).<sup>16–18</sup> Pknox1 forms an active ternary complex with HoxB1 and Pbx proteins, crucial for the activation of *HoxB2* transcription.<sup>19</sup>

The Pknox1 interactome has been isolated and includes motor proteins such as non-muscle myosin II A (NMMIIA) and

\*Correspondence to: Gabriela Naum-Onganía; Email: gnaum@conicet.gov.ar  
Submitted: 04/24/2013; Revised: 12/23/2013; Accepted: 12/27/2013

Citation: Naum-Onganía G, Díaz-Cortez VM, Blasi F, Rivera-Pomar R. Nuclear actin polymerization from faster growing ends in the initial activation of Hox gene transcription: Are nuclear speckles involved?. *Transcription* 2013; 4:258–270; PMID: 24406343; <http://dx.doi.org/10.4161/trns.27672>

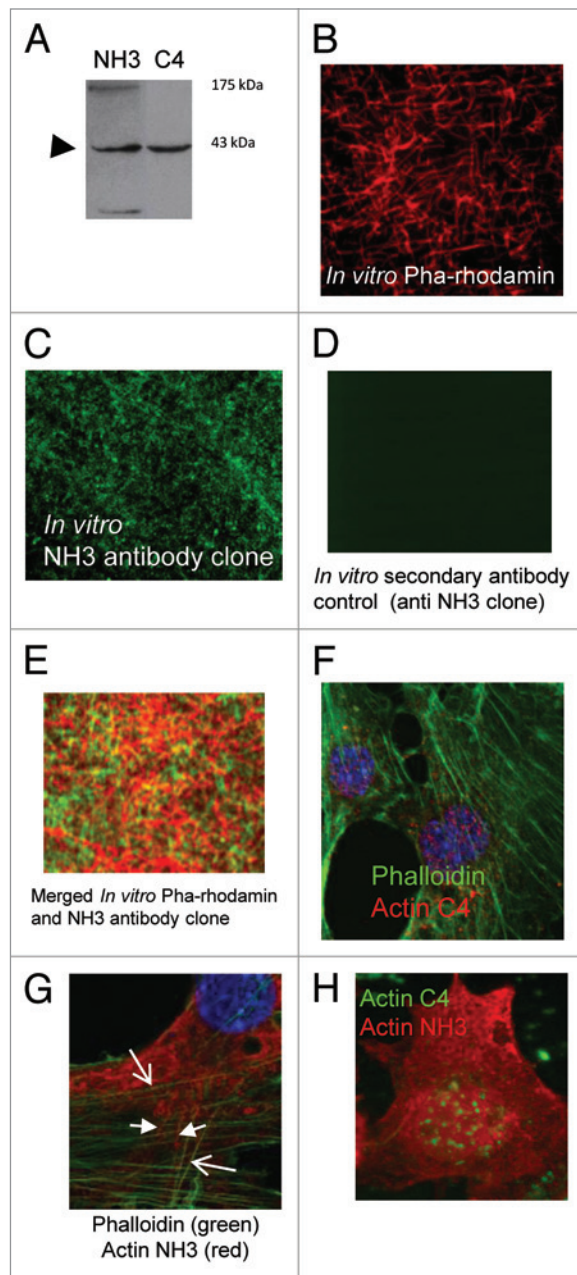


**Figure 1.** Anti-F-actin antibody validation (Abcam ab205, NH3 clone). **(A)** The immunoblot of nuclear extracts from NT2-D1 cells is shown. Both anti-F-actin antibody (NH3 clone) and anti-G-actin antibody (C4 clone) detect a band of similar molecular weight (43 kDa), which corresponds to actin. **(B)** In vitro actin polymerized filaments stabilized with phalloidin rhodamin are shown in red (In vitro Pha-rhodamin). **(C)** In vitro polymerized actin oligomers (In vitro NH3 clone) are shown in green, and stained with the primary antibody: the NH3 antibody clone. After that, a secondary antibody conjugated to fluorescein (FITC) was used. **(D)** Control showing polymeric actin incubated with the secondary antibody conjugated to fluorescein (FITC, background). **(E)** Partial co-localization between in vitro polymerized actin filaments (Pha-rhodamin, red) and the actin NH3 antibody clone (Actin NH3, green). **(F)** NIH-3T3 cells treated with a buffer for actin filaments stabilization. F-actin was dyed in green with phalloidin-FITC and in red with the C4 antibody clone. **(G)** NIH-3T3 cells treated with a buffer for actin filaments stabilization. F-actin was dyed in green with phalloidin-FITC (arrows). The NH3 antibody clone was dyed in red (head arrows). **(H)** A type NT2-D1 cell stained with both antibodies is shown (Actin NH3 is shown in red; Actin C4 in green). Notice that they dye different types of actin: the NH3 clone identifies a pattern similar to the cytoskeleton and the C4 clone detects actin aggregates.

recruitment of actin monomers, consequently delaying the process.<sup>28</sup> The action of these actin-interfering drugs results in a general transcription inhibition suggesting the role of actin filaments in the process.<sup>27</sup>

In previous work, we have shown that nuclear actin polymerization is involved in the induction of *HoxB* gene expression.<sup>29</sup> Here, we suggest the existence of a narrow time frame for the inhibition of *HoxB* transcription, and propose a model in which nuclear actin polymerization might be involved in the initial activation of co-transcriptional splicing events coordinating the expression of the cluster. The initial activation should involve the movement of the cluster from a non-active chromosomal territory into transcriptional/splicing active compartments—the nuclear speckles—for proper gene expression. In our model, polymeric nuclear actin and other nuclear factors are the molecular driving motor that brings the *HoxB* cluster into the nuclear speckles.

## Materials and Methods

### Cell cultures

Human NT2-D1 cells were grown in DMEM (Cambrex BioScience, Milan, Italy) and used at 70% confluence. *Trans-retinoic acid* was from Sigma-Aldrich (Milan, Italy). Controls were treated with 0.1% DMSO. Actin-interfering drugs (cytochalasin D and latrunculin A) were from EMD Bio-sciences (Darmstadt, Germany). NT2-D1 cells were treated with 1  $\mu$ M RA to obtain an 80–100% S phase cell population.<sup>30</sup> Cells morphology was controlled by choosing grouping cells spreading on large adhesive patches, which indicates that the probability of entering in S phase is about of 90%.<sup>31</sup>

### Treatments

Actin-interfering drugs (toxins) were added to the medium containing retinoic acid (RA) at different times (for further clarification, see Fig. S2, which presents a sketch of the treatments). RA was added to the cells at 0h time point for 16, 48 and 72 h (16h RA-, 48h RA- and 72h RA-treatments, respectively). Control cultures were treated with DMSO. Cytochalasin D (100nM) or

$\gamma$ - and  $\beta$ -actin in the nuclear, but not in the cytosolic Pknox1 complex.<sup>20</sup>  $\beta$ -actin is part of the chromatin remodeling complex<sup>21</sup> and is important for the activity of RNAP I, II and III.<sup>22–24</sup> Thus, it can be hypothesized that Pknox1 and  $\beta$ -actin are involved in transcription. Moreover, the actin polymerization inducer, N-WASP, and its activator Arp2/3 are also bound to RNAP II and transcription/splicing factors p54<sup>(nrb)</sup> and PSF. Both N-WASP and Arp2/3 are required for RNAP II-dependent transcription.<sup>25,26</sup>

Globular and polymeric forms of actin (G- and F-actin, respectively) are in the nucleus in a balanced equilibrium.<sup>27</sup> Cytochalasin D (CytD) inhibits actin filament polymerization from the faster growing ends (plus ends), whereas latrunculin A (LatA) does so by unbalancing the polymerization reaction between globular and polymeric species by means of the

latrunculin A (50nM) were added separately at 0h time point for the 16 RA-treatment, at 24h time point for the 48h RA-treatment and at the 48h time point for the 72h RA-treatment. Moreover, a 19h RA-treatment was performed. In this case, the toxins were added at the 3h time point and remained in the cultures for 16 h, so that these cultures remained free of toxins for 3 h. The *HoxB* gene transcript levels were measured by quantitative RT-PCR (RT-q-PCR) at the end of RA-treatments (16, 20, 48 and 72 h).

#### Antibodies

The following antibodies were used: purified mouse anti-actin monoclonal antibody (anti-G-actin, by Cedarlane, C4 clone), monoclonal anti-F-actin antibody (Abcam205, NH3 clone), polyclonal anti-total RNAP II (N-20: sc-899, from Santa Cruz Biotechnologies) and anti-Ser2P (MMS-129-RA) from Covance; monoclonal anti-N-WASP (Santa Cruz Biotechnology, Santa Cruz, CA); monoclonal anti-Prep-1 (Santa Cruz Biotechnology, Santa Cruz, CA) and polyclonal antibodies of Prep1 (Pknx1). Polyclonal anti-PSF and monoclonal anti-p54<sup>nrb</sup> antibodies were kind gifts from Drs. A. Krainer (Cold Spring Harbor Laboratory, Cold Spring Harbor, NY) and J. Patton (Vanderbilt University, Nashville, TN), respectively. Donkey anti-mouse-FITC and donkey anti-mouse-TRITC were from Jackson. Monoclonal goat anti-mouse IgM-FITC was from Zymed Laboratories Inc. Phalloidin-rhodamin from Jackson was used for the in vitro actin polymerization assay.

#### Confocal immunofluorescence

For immunofluorescence of permeabilized NT2-D1 cells, monolayers plated on poly-(lysine)-coated coverslips were fixed with 4% paraformaldehyde in PBS at 4 °C for 10 min, washed and quenched with 0.1 M glycine. The NIH-3T3 cells were treated with a potassium-rich buffer (K 0.1 M) prior to their fixation with 4% of paraformaldehyde (PFA), for the stabilization of actin filaments. Primary antibodies against G-actin, F-actin and Pknx1 were diluted in a 1% bovine serum albumin (BSA) and 0.1% Triton, and applied onto coverslips for 1h at room temperature. After thorough washing, cells were labeled with secondary antibodies conjugated to fluorophores and with 4',6-diamidino-2-phenylindole (DAPI). All cell samples were analyzed in a PerkinElmer UltraView ERS spinning disk confocal microscope (PerkinElmer Life and Analytical Sciences, Shelton, CT) with an oil immersion objective 63x, 1.4 NA. Morphometric analysis of immunostained monolayers was performed by the ImageJ Program (see Fig. S1). To quantify co-localization, the *ImageJ plugin co-localization software* was used (ratio [0–100%] = 80; threshold-channel-red [0–255] = 50 or 100; threshold-channel-green [0–255] = 50 or 100; and display-value [0–225] = 255).

#### In vitro actin polymerization assay

Rhodamin-labeled actin and rabbit skeletal muscle actin were purchased from Cytoskeleton, Inc. Unlabeled actin was polymerized at 5 μM in buffer F (10 mM TRIS-HCl, pH 7.5, 100 mM KCl, 2 mM MgCl<sub>2</sub>, 1 mM ATP, 0.2 mM EGTA, and 0.2 mM DTT) for 1 h. For assembly from F-actin seeds, a 15-μl aliquot of preassembled unlabeled actin filaments was incubated with buffer G containing 0.2 mM ATP and plated onto a coverslip. Actin filaments were visualized in a fluorescence microscope. For the incubation of the filaments with the antibody by AbCam, actin

polymerization was performed without rhodamin, and polymers were incubated with this antibody for 1 h. Next, polymers were incubated with the fluorescein-conjugated secondary antibody for 1 h (goat anti-mouse IgM-FITC antibody), plated onto a coverslip and visualized in a fluorescence microscope.

#### RNA and protein extraction, and quantitative real-time PCR

RNA was extracted with Qiagen mini columns and RNeasy mini kit-250 (Qiagen GmbH, Hilden, Germany). Nuclear extracts were prepared as described in Dignam et al.<sup>32</sup>

RNA, 1 μg, oligodT, 0.5 μg, and SuperScript First-Strand Synthesis System for RT-PCR kit (Invitrogen) were used. Primers were as follows: GAPDH: ACCACCTGGT GCTCAGTGTA (sense) and ACATCATCCC TGCCTCTACTG (antisense); HoxB1: GCATCTCCAG CTGCCTCCTT (antisense) and CCTTCTTAGA GTACCCACTCTG (sense); and HoxB2: AGTGGAATTC CTTCTCCAGTTCC (antisense) and TCCTCCTTTC GAGCAAACCTTCC (sense). cDNA, 5 ng, was amplified (in triplicate) with TaqMan PCR Mastermix and TaqMan Gene expression assay (Applied Biosystems, Foster City, CA) and measured in the ABI/Prism 7900 HT Sequence Detector System (Applied Biosystems), using a pre-PCR step of 10 min at 95 °C, 40 cycles of 15 s at 95 °C and 60 s at 60 °C. RNA without reverse transcriptase was used as negative control. 18S rRNA and GAPDH were used as standards. Proprietary primers from Applied Biosystems were used. For real-time PCR of the *HoxB2* expression levels in actin mutant transfections, the reverse-transcribed RNA was amplified in a light cycler (Roche, Indianapolis, IN) using a FastStart DNA mix SYBR Green I kit (Roche). PCR conditions were as follows: for *HoxB2* mRNA: denaturation and DNA polymerase activation step, 95 °C for 10 min; second denaturation step, 95 °C for 15 s; annealing step, 56 °C for 6 s; and extension step, 72 °C for 20 s. GAPDH conditions were as follows: first denaturation and DNA polymerase activation step, 95 °C for 10 min; second denaturation step, 95 °C for 15 s; annealing step, 57 °C for 6 s; extension step, 72 °C for 20 s. The amount of *HoxB2* mRNA was normalized to *GAPDH* mRNA. The primers are reported above.

#### Co-immunoprecipitation

Co-IPs from nuclear extracts of NT2-D1 cells were performed with protein G-Sepharose (Zymed Laboratories, San Francisco, CA). Nuclear proteins (1 mg of endogenous protein) were diluted in 10 mM Tris buffer pH8, 0.2% NP-40 and 150 mM NaCl and pre-cleared. Then, they were incubated with 5 μg of anti-rabbit PSF antibody (α-PSF) overnight at 4 °C and pulled down with protein G. Immunoblots were incubated with anti-Pknx1, anti-THOC and anti-C4 antibodies. A non-relevant antibody (anti-uPA) was used as control (α-Ctrl).

#### Tandem Affinity Purification

TAP technique was performed with the Pknx1-TAP vector in two non-denaturing steps: i) binding to an IgG matrix and elution with the TEV protease ii) purification with calmodulin-coated beads in the presence of calcium. Retrovirus infection: Cells were infected using a retrovirus produced in Phoenix ectropic packaging cells and selected with puromycin. N and C extraction: Cells expressing Pknx1-TAP were lysed to obtain

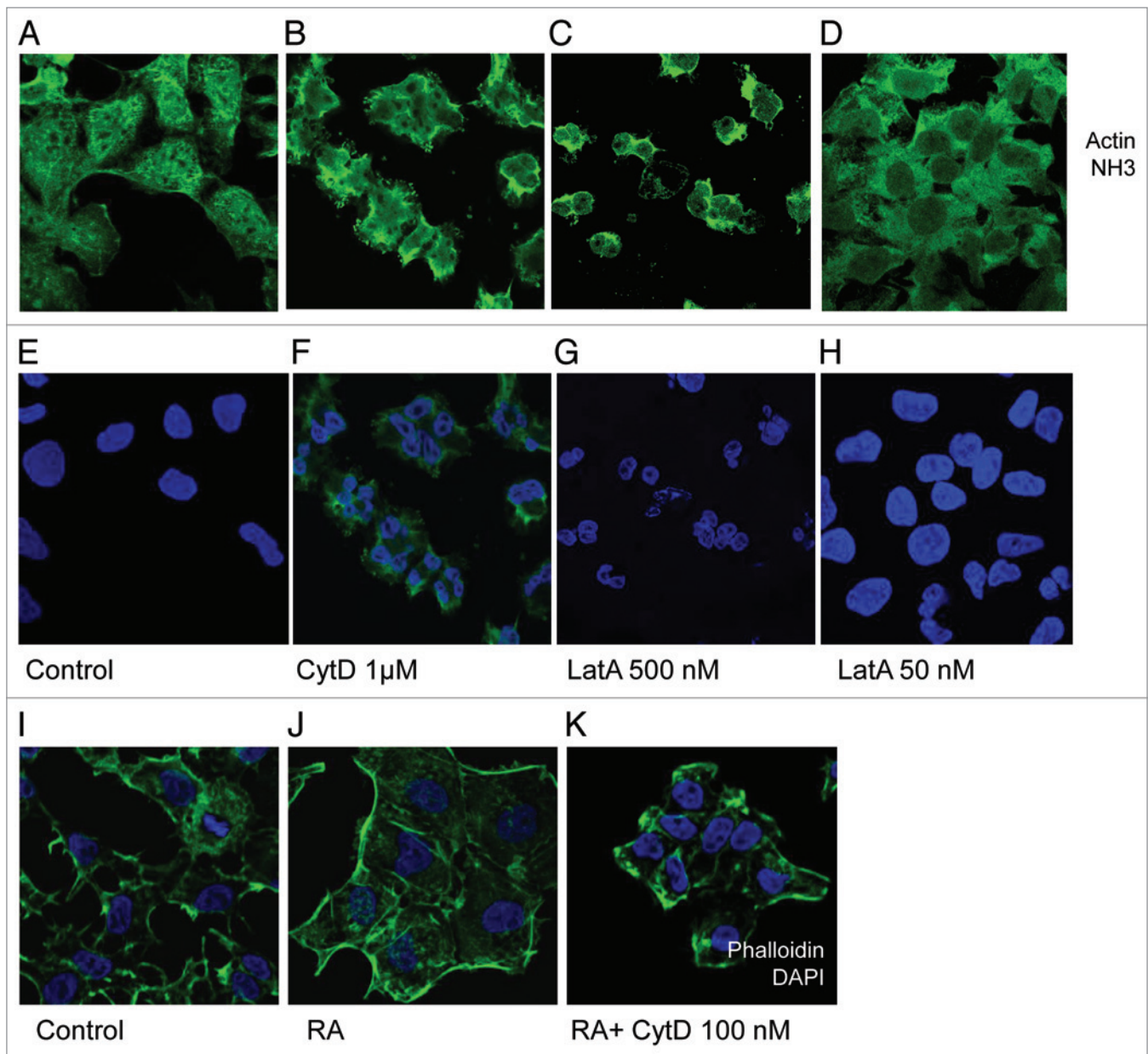


**Figure 2.** The Anti-F-actin antibody detects polymeric actin in the nucleus of NT2-D1 cells. Confocal immunofluorescence shows NT2-D1 cells stained with the NH3 antibody clone (Actin NH3, green) or with phalloidin (green). Control cells are shown in panels **A**, **E** and **I**. Dyed polymeric actin with the NH3 antibody is present in the nuclei of control cells (**A**), which were stained in blue with DAPI (**E**). Cells were treated either with CytD 1 μM (**B** and **F**) or LatA 0,5 μM (**C** and **G**). Notice that cytoplasm contract (**B** and **C**) and that nuclear fluorescence corresponding to dyed polymeric actin shows a decrease (**B–D**), suggesting that nuclear actin is depolymerized. NT2-D1 cells were treated either with RA or with RA plus 100 nM of CytD and stained with phalloidin (**I–K**, green). Notice also that cytoplasm shows retraction but nuclei do not.

nuclear (N) and cytoplasmic (C) fractions. Lysates were resuspended in buffer A (10 mM HEPES KOH pH 7.9, 1.5 mM MgCl<sub>2</sub>, 10 mM KCl, 0.5 mM DTT plus a cocktail of protease inhibitors) and with 1/30 of the volume of 10% Triton x-100. Cell extracts were centrifuged for 1min at 11000 rpm. The resulting nuclear pellets were treated with buffer C (20 mM HEPES pH 7.8, 25% glycerol, 420 mM NaCl, 1.5 mM MgCl<sub>2</sub>, 0.2 mM EDTA plus protease inhibitors) for 30 min at 4 °C and centrifuged at 13000 rpm during 15 min. Supernatants were nuclear (N) and cytoplasmic (C) fractions. The last (C) was treated with

0.11 volume of buffer B (0.3 M HEPES pH 7.9, 1.4 M KCl, 30 mM MgCl<sub>2</sub>), rotated for 30 min at 4 °C and centrifuged for 15 min at 13000 rpm. IgG binding: Both N and C extracts were adjusted to IgG-binding conditions (IBB buffer: 10 mM TRIS-HCl at pH 8, 0.2% NP-40, 150 mM NaCl), incubated in batch with IgG beads (Amersham Biosciences) and rotated O.N. at 4 °C. TEV cleavage: After washing with IBB buffer and with TEV cleavage buffer (TCB: 10 mM TRIS-HCl at pH8, 150 mM NaCl, 0.2% NP-40, 0.5 mM EDTA, 0.5 mM DTT), TEV cleavage was performed by incubation with TCB and AcTEV

protease (10 U/μl) (Invitrogen) for 2h on a rotator shaker at 16 °C. Calmodulin binding and elution: TEV eluate treated with CaCl<sub>2</sub> and CBB buffer (50 mM TRIS-HCl pH8, 150 mM NaCl, 1 mM Mg-acetate, 1 mM imidazole, 4 mM CaCl<sub>2</sub>, 0.2% NP-40, 10 mM β-mercaptoethanol) was added and mixed with calmodulin beads (Stratagene) at 4 °C. Calmodulin beads were washed with CBB and boiled with 2X Laemmli buffer.

## Results and Discussion

### Validation of monoclonal antibodies to study polymeric nuclear actin

The human teratocarcinoma cell line (NT2) is an embryonic multipotent line that, upon RA treatment, differentiates into a variety of cell types.<sup>33</sup> The NT2-D1 clone is an excellent model to test the role of nuclear actin polymerization in the RA-induced expression of the *HoxB* cluster genes.<sup>12</sup> To analyze this, we determined the presence of polymerized actin by immunocytochemistry. For this purpose, we first determined the specificity of the antibodies used to detect both G- and F-actin, namely C4 and NH3 antibody, respectively. They detect an immunoreactive protein of 42 kDa that corresponds to actin, as judged by its molecular weight (Fig. 1A). We then assayed the antibodies against in vitro polymerized actin, which is readily detected using labeled phalloidin (Fig. 1B) (for details on in vitro polymerization assay see Methods). According to this, immunocytochemistry has shown that in vitro polymerized actin filaments are recognized by the NH3 antibody clone (Fig. 1C). This reaction is specific as the secondary antibody alone does not detect any actin (Fig. 1D) and taking into account that the only protein present in the preparation is actin, the different reactivity might reflect different actin structures. In this sense, both phalloidin-rhodamin and the NH3 antibody clone co-localize partially in the in vitro actin preparation (Fig. 1E), implying that there could be a competition between phalloidin and the NH3 antibody for F-actin. In addition, we have confirmed that the C4 clone detects protein aggregates in actin filament stabilized-NIH-3T3 cells, whereas phalloidin and the NH3 clone detect actin filaments (Fig. 1F and G, respectively). Furthermore, the C4 clone did not show any reaction against in vitro polymerized actin filaments (not shown), suggesting that it does not detect F-actin. In summary, we conclude that the NH3 antibody is a suitable tool for F-actin detection.

In order to validate the results in our system of study, we performed immunocytochemistry in NT2-D1 cells with the C4 and NH3 antibody clones. As we have noticed, both antibodies show different staining patterns (Fig. 1H). The NH3 antibody identifies a pattern of actin similar to the cytoskeleton, whereas the C4 antibody detects discrete spots in the nucleus (speckles). Therefore, we conclude that we are able to distinguish different types of actin structures and that monoclonal anti-F-actin antibody is a valid tool to study polymeric nuclear actin in NT2-D1 cells.

It is known that collinear *HoxB* activation requires DNA replication (S phase of the cell cycle).<sup>34</sup> Thus, to determine whether the effects on *HoxB* expression are specific to actin-interfering drugs and do not reflect an indirect effect on cell

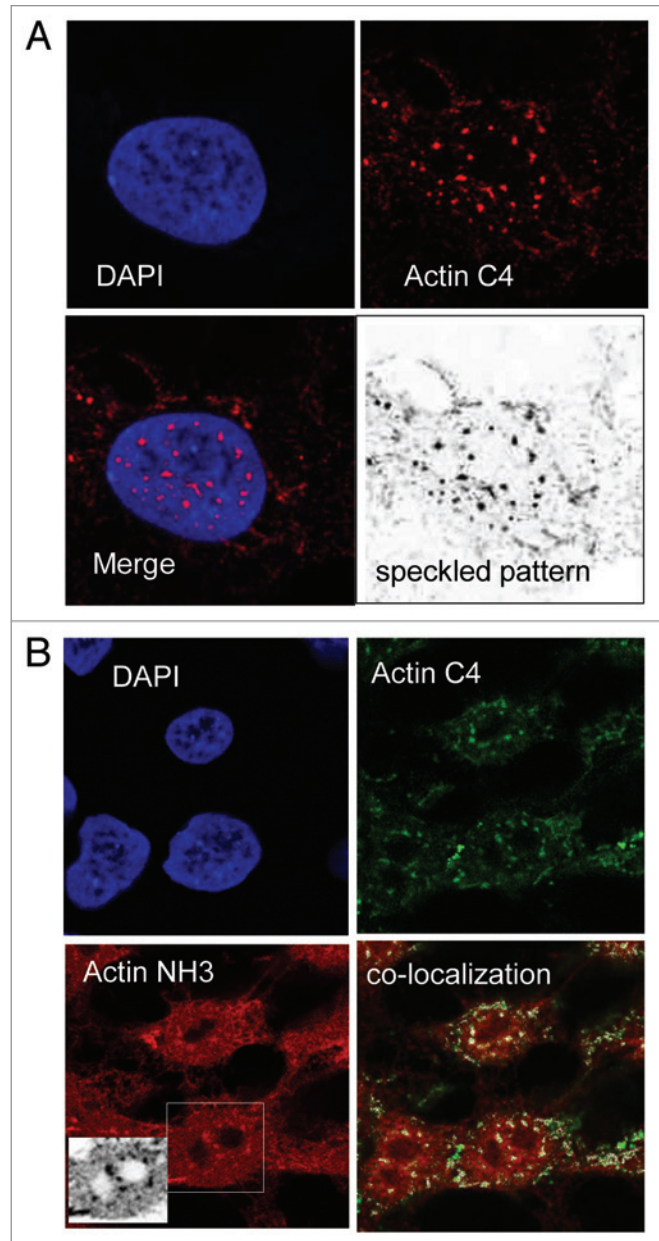


**Figure 3.** Actin shows a nuclear speckled pattern in NT2-D1 cells. (A) NT2-D1 cell nucleus stained with DAPI (blue) is shown at high magnification (63X magnification plus a 4X confocal microscope software zoom). Actin accumulates in defined spots (red), which match lower density chromatin areas (euchromatic regions) in the DAPI staining. These regions could correspond to interchromatic spaces (speckled pattern) and the aggregates to nuclear speckles. (B) Morphometric analysis of immunostained monolayers performed by the ImageJ Program. DAPI staining is shown in blue. Actin detected by the C4 clone is shown in green (Actin C4) and actin detected by the NH3 clone is shown in red (Actin NH3). Co-localization between both types of actin is shown (white pixels). To quantify co-localization between them, the *ImageJ* plugin *co-localization* software was used. Notice that actin stained by the NH3 antibody clone (anti-F-actin antibody) occurs in the peripheral area inside the nucleus, but accumulates in the interchromatic spaces (see black and white sub-panel).

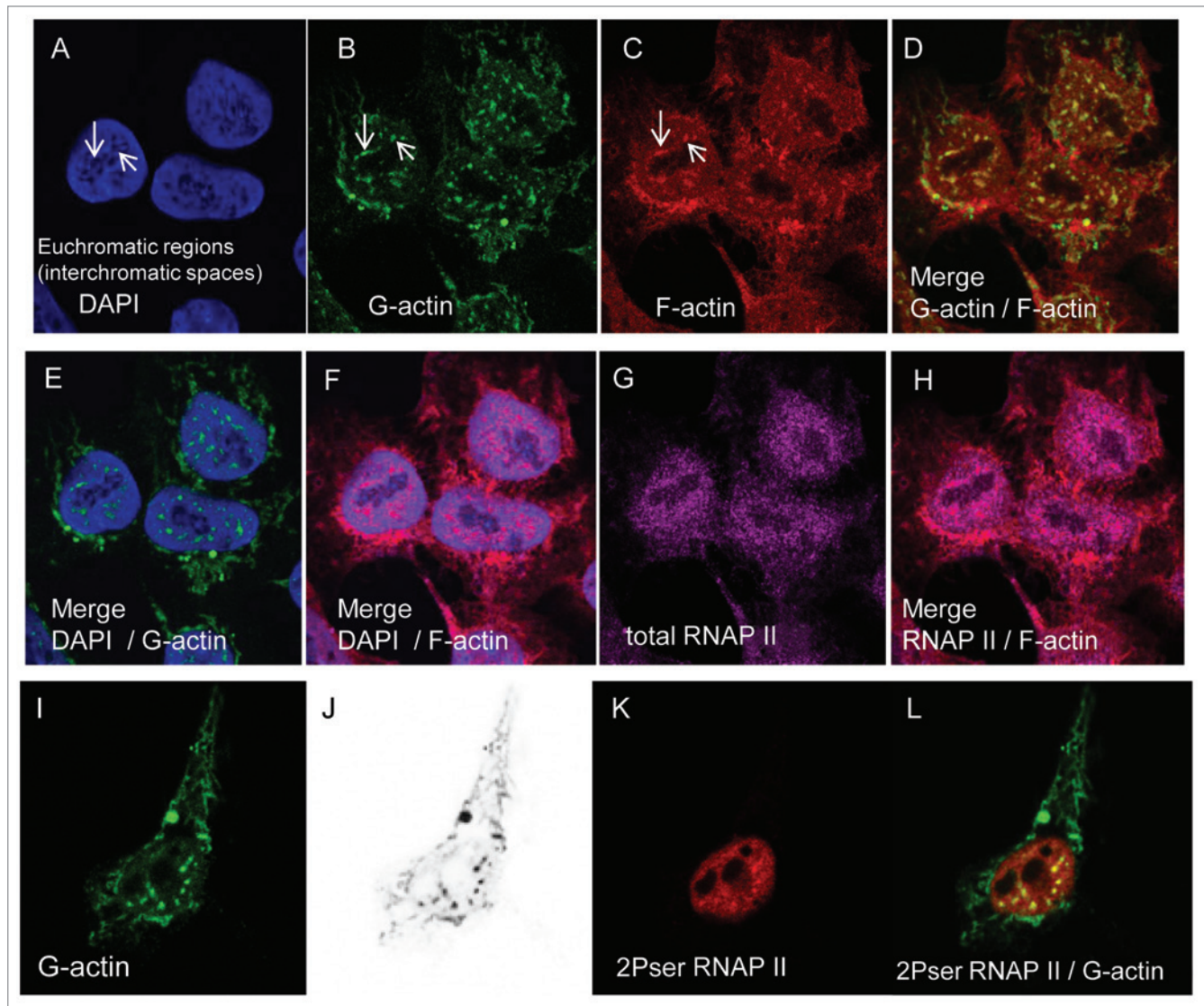


**Figure 4.** Nuclear actin co-localizes with the elongating RNAP II in a speckled pattern. NT2-D1 cell nuclei stained with DAPI are shown at high magnification. In the DAPI staining, the euchromatic regions or interchromatic spaces are indicated (A, arrows). Globular actin detected by the Actin C4 antibody (onwards G-actin) accumulates in defined spots (B), which match the aforementioned spaces (E). Polymeric actin detected by the Actin NH3 antibody (onwards F-actin) is placed in the peripheral area inside the nucleus and accumulates in the mentioned regions (C and F). Notice that G- and F-actin co-localize in the interchromatic spaces (D, yellow speckles). Total RNA polymerase II (G) co-localizes with F-actin in the NT2-D1 nuclei (H) whereas the active form of RNAP II (2Pser RNAP II) co-localizes with G-actin aggregates (I–L). As it is shown, G-actin co-localizes with the elongating RNAP II in a speckled pattern (J and L).

cycle, S phase-NT2-D1 cells were analyzed. For this purpose, we used RA (1  $\mu$ M)-treated cells (see Methods). Then, we used cytochalasin D (CytD) and latrunculin A (LatA) to inhibit actin polymerization and studied their effect on nuclear actin polymerization with the NH3 antibody. Compared with controls, after high CytD and LatA concentrations, NT2-D1 cells shrunk in size (cytoplasm and nucleus) (Fig. 2A–C and E–G), which confirms that the inhibitors interfered with actin polymerization in vivo. Nevertheless, the fact that nuclei did not shrink at the used concentrations (CytD 100 nM or LatA 50 nM) suggests that they were appropriate to study transcription (Fig. 2E–H and Fig. 2I–K). Remarkably, the inhibition of actin polymerization was also evident in the nuclei of NT2-D1 cells because NH3

antibody fluorescence decreased after CytD and LatA treatments (Fig. 2B–D). However, this effect has not been observed using the C4 antibody (data not shown). In summary, these results show that F-actin is present in the nucleus of NT2-D1 cells and behaves as cytoplasmic actin.

#### Nuclear actin polymerization occurs in nuclear speckles

We have shown by confocal microscopy that nuclear actin presents a punctate nuclear pattern that is usually termed as speckled pattern (Fig. 3A). This pattern could also be observed in cells labeled with the NH3 antibody (Fig. 3B, Actin NH3). We have found that the C4 antibody clone detects actin aggregates (onwards called G-actin) in the nucleus of NT2-D1 cells. Remarkably, as co-localization between both anti-actin

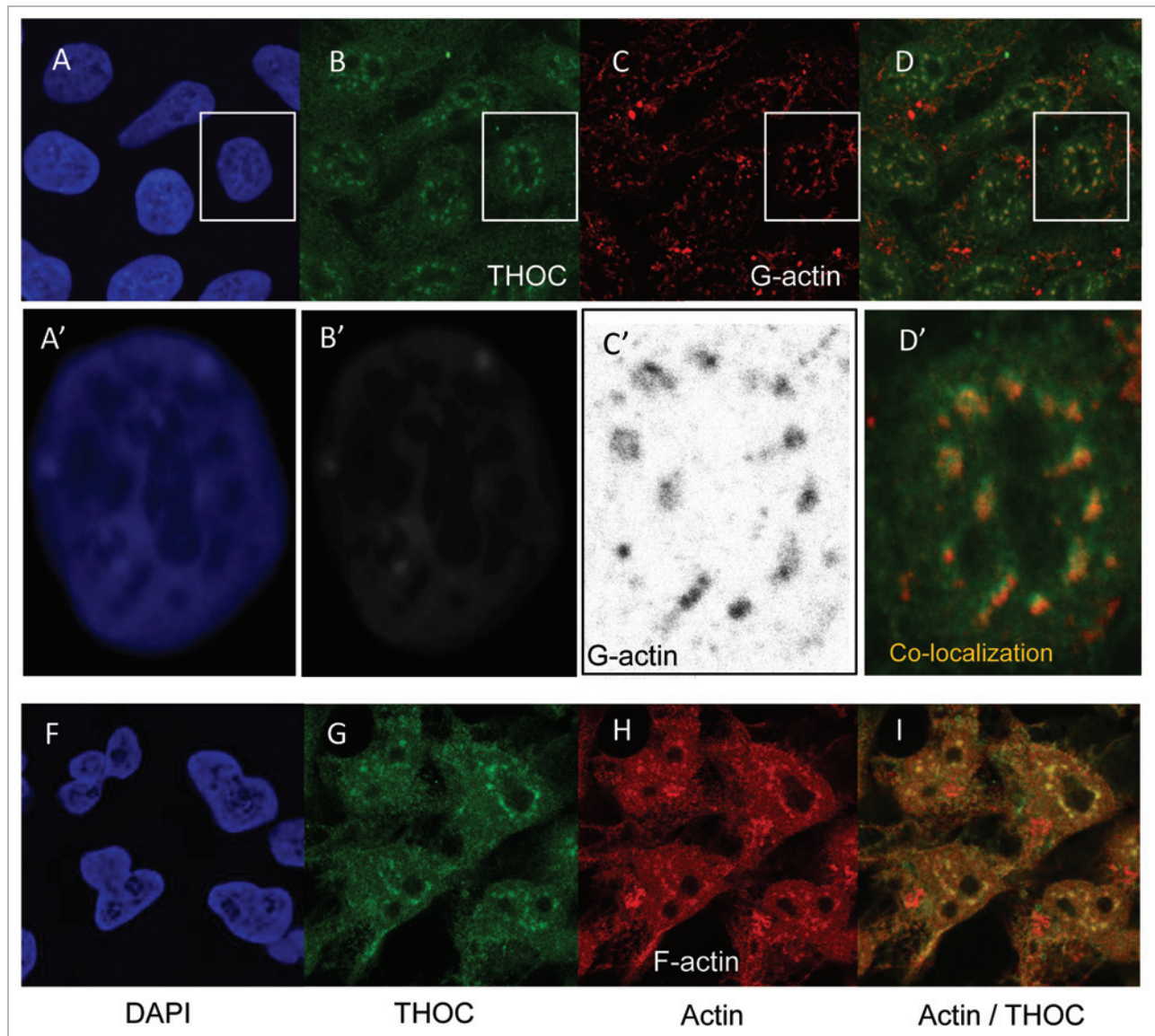


**Figure 5.** G- and F-actin co-localize with the mRNA elongation factor in nuclear speckles. G-actin speckles match euchromatic regions (interchromatic spaces) where co-localize with the mRNA elongating factor, hHrp1/p84/Thoc1 (THOC) (panels **A–D** and at high magnification, **A'–D'**). Notice the interchromatic spaces around the central region of the nucleus (**A'** and **B'**). Although THOC (**G**) and F-actin (**H**) show a partial co-localization pattern both in nucleus and in cytoplasm (**I**, orange) co-localization speckles accumulate around the central region in an evident speckled pattern (**I**, yellow).

antibodies was observed in these regions, we further analyzed the nature and morphology of the aggregates, which appear as discrete spots or speckles (Fig. 3A and B, Actin C4).

G-actin aggregates match less dense chromatin areas as judged by the weaker DAPI staining in the most peripheral region within the nucleus, which is a sign of euchromatin or spaces between heterochromatin (interchromatin space; see Fig. 3A, and Fig. 4A, B, E). A more detailed evaluation has shown that not only G-actin but also F-actin matches these regions (Fig. 3B and Fig. 4A–E) co-localizing in them (Fig. 4D)—G-actin as speckles and F-actin as a cytoskeleton-like network (Fig. 4B and C). Co-localization suggests that the process of actin polymerization might take place in these speckles. Considering that G-actin speckles coincide with euchromatin, we investigated the

localization of the elongating form of RNAP II (2Pser RNAP II), an indicator of transcriptional activity. Whereas total RNAP II localizes both in nucleus and cytoplasm (Fig. 4G and H), 2Pser RNAP II is enriched in the speckles where G-actin is present. As we can see, both 2Pser RNAP II and G-actin co-localize in these nuclear structures (Fig. 4K and L).

To provide additional evidence, we analyzed the co-localization between nuclear actin and the hHrp1/p84/Thoc1 (THOC)—also marker of the nuclear matrix. This protein is known to localize in splicing speckles<sup>35,36</sup> and is a subunit of the evolutionarily conserved TREX complex (transcription/export). THOC is an mRNA elongation factor that has been implicated in many stages of RNA processing, coupling transcription elongation to the nuclear export of mRNAs. In humans, it associates

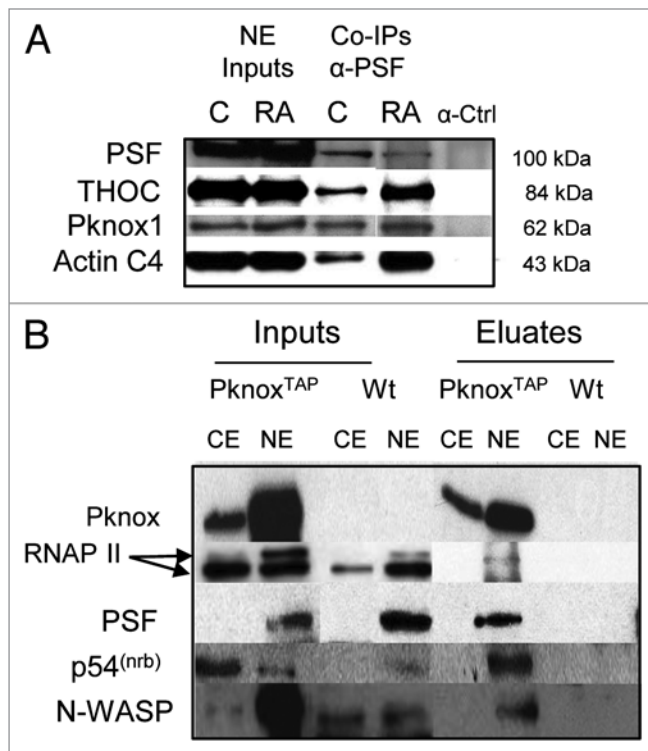


**Figure 6.** Pknox1 protein complex composition. **(A)** Co-immunoprecipitations (Co-IPs) with the endogenous transcription/splicing factor PSF. Nuclear extracts (NE) of control (C) and retinoic acid-NT2-D1 treated cells (RA) were used. The same membrane was sequentially incubated with the anti-Pknox1, anti-THOC and anti-C4 antibodies. The uPar protein, which does not co-IP with PSF was used as negative control ( $\alpha$ -Ctrl). **(B)** Lysate cultures (inputs) and TAP eluates (extracts from infected cells with the *Pknox1<sup>TAP</sup>* construct), were isolated from two independent experiments and analyzed by western blot. Nuclear (NE) and cytoplasmic (CE) extracts from cells infected with the *Pknox1<sup>TAP</sup>* virus and nuclear and cytoplasmic extracts from wild type cells (Wt) are shown. Lanes for wild type extracts correspond to cultures without any vector (not infected). Membranes were sequentially incubated with the anti-RNAP II, anti-p54<sup>(nr)</sup>, anti-PSF and anti-N-WASP antibodies. Phosphorylated RNAP II, PSF, p54<sup>(nr)</sup> and N-WASP were purified with Pknox1 in the nuclear *Pknox1<sup>TAP</sup>* eluates.

with the 2Pser RNAP II, RNA processing factors, and unspliced pre-mRNAs (but not spliced mRNAs).<sup>35-37</sup>

In this work, we have found that G-actin co-localizes with the splicing speckles protein THOC (Fig. 5A–D). Although F-actin shows partial co-localization with THOC (Fig. 5I, orange), co-localization speckles accumulate around the central region of the nucleus in an evident yellow speckled pattern (Fig. 5I). In summary, our results show that G-actin aggregates correspond to nuclear speckles and co-localize with F-actin, suggesting that nuclear actin polymerization might occur in these nuclear bodies. Therefore, polymeric nuclear actin might be involved in RNA processing as mRNA elongation, splicing and mRNA export.

#### Retinoic acid induces co-localization between Pknox1 and polymeric actin in nuclear speckles

We have recently shown that transcription of the *HoxB* genes that are closer to the 3' end of the cluster (proximal genes, i.e., *HoxB1/B2*) is N-WASP-dependent and that the DNA-binding

Pknox1-Pbx1 complex is constitutively associated with p54<sup>(nr)</sup>.<sup>29</sup> This transcription/splicing factor associates with the actin polymerization inducer, N-WASP.<sup>25</sup>

By chromatin immunoprecipitation experiments (ChIP), we demonstrated that  $\beta$ -actin and N-WASP bind the *HoxB2* enhancer in NT2-D1 cells, only after RA treatment.<sup>29</sup> Even though ChIP experiments did not reveal polymeric actin bound to DNA, this cannot be ruled out. Thus, it would be plausible that RA might induce polymeric nuclear actin interaction with Pknox1 for the movement of the *Hox* cluster to undergo the transcription/splicing process.

N-WASP and  $\beta$ -actin bind the *HoxB2* enhancer together with Pknox1, the elongating form of RNAP II, and transcription/splicing factors p54<sup>(nr)</sup> and PSF.<sup>29,38,39</sup> In addition, both p54<sup>(nr)</sup> and PSF bind the C-terminal domain of the largest subunit of the RNAP II, and can interact directly with the 5' splice site, indicating that these factors may mediate contacts between RNAP II and snRNPs during the coupled transcription/splicing process.<sup>40,41</sup> Furthermore, PSF stimulates 3' end cleavage in the absence of pre-mRNAs splicing and requires the RNAP II C-terminal domain for stimulating the pre-mRNA processing.<sup>42</sup> P54<sup>(nr)</sup> associates with the 5' splice site within large complexes.<sup>41</sup> Therefore, it could act in concert with  $\beta$ -actin, N-WASP and the Pknox1-Pbx1 dimer for the transcription/splicing process, connecting RNAP II with the polymeric nuclear actin system.

Because NT2-D1 cells have a high level of endogenous PSF in the nucleus, we used the anti-PSF antibody to pull down transcription/splicing complexes as a first approach. With this technique, we found that Pknox1, THOC and G-actin were pulled down by the PSF-antibody from nuclear extracts of NT2-D1 untreated cells (Fig. 6A and C lanes). As we notice, the nuclear levels of Pknox1, THOC and G-actin have not changed under the RA effect (inputs). However, the interaction between the splicing speckle factor THOC and G-actin seems to increase with RA (Fig. 6A, RA lanes), suggesting that it might enhance this interaction.

To further check the identity and specificity of proteins that interact with Pknox1 we used the tandem affinity purification (TAP) technique. We prepared nuclear and cytoplasmic extracts from cells expressing the *Pknox1<sup>TAP</sup>* construct and non-expressing control cells. In nuclear extracts, Pknox1 co-purified with N-WASP, p54<sup>(nr)</sup>, PSF and 2Pser RNAP II (Fig. 6B). It can be noticed that the lower band in the RNAP II panel corresponds to the total polymerase that is observed by confocal microscopy both in nucleus and cytoplasm (see Fig. 4 panels G and H). As we observe, nuclear and cytoplasmic Pknox1 could not be purified from control cells due to the low level of endogenous Pknox1. The same results have been observed in cells infected with empty vector (not shown).

We then investigated, by confocal microscopy, whether the Pknox1 interactors were linked to nuclear polymeric actin. Upon RA induction, Pknox1 co-localized with F-actin in a speckled pattern (Fig. 7G); however, this pattern has not been observed before the RA treatment (Fig. 7A), suggesting that nuclear polymeric actin could be the component of such a complex involved



**Table 1.** Cytochalasin D and Latrunculin A effect on the RA-induced *HoxB* gene collinear expression

Genes	RA								
	16h	16h + CytD t = 0h	16h + LatA t = 0h	48h	48h + CytD t = 24h	48h + LatA t = 24h	72h	72h + CytD t = 24h	72h + LatA t = 24
<b>HoxB1</b>	<b>1.0</b> (1.22–0.82)	<b>0.177</b> (0.21–0.15)	<b>0.92</b> (1.05–0.81)	<b>1.0</b> (1.07–0.94)	<b>0.996</b> (1.02–0.97)	<b>0.93</b> (1.04–0.83)	<b>1.0</b> (1.22–0.82)	<b>0.633</b> (0.75–0.54)	<b>1.07</b> (1.249–0.917)
<b>HoxB2</b>	<b>1.0</b> (1.052–0.951)	<b>0.05</b> (0.061–0.041)	<b>0.86</b> (1.097–0.673)	<b>1.0</b> (1.12–0.89)	<b>1.0</b> (1.12–1.08)	<b>0.65</b> (0.79–0.53)	<b>1.0</b> (1.14–0.876)	<b>1.1</b> (1.22–1.095)	<b>1.154</b> (1.216–1.095)
<b>HoxB3</b>	<b>UN</b>	<b>UN</b>	<b>UN</b>	<b>1.0</b> (1.19–0.84)	<b>0.5</b> (0.62–0.40)	<b>0.49</b> (0.68–0.35)	<b>1.0</b> (1.2–0.83)	<b>0.72</b> (0.82–0.63)	<b>0.8</b> (0.93–0.689)
<b>HoxB4</b>	<b>UN</b>	<b>UN</b>	<b>UN</b>	<b>1.0</b> (1.22–0.82)	<b>0.92</b> (1.08–0.78)	<b>0.7</b> (0.76–0.875)	<b>1.02</b> (1.25–0.80)	<b>0.885</b> (1.05–0.74)	<b>0.811</b> (0.896–0.735)
<b>HoxB5</b>	<b>UN</b>	<b>UN</b>	<b>UN</b>	<b>1.02</b> (1.22–0.82)	<b>0.985</b> (1.11–0.88)	<b>0.5</b> (0.62–0.4)	<b>1.0</b> (1.09–0.92)	<b>1.035</b> (1.17–0.92)	<b>0.89</b> (0.938–0.845)
<b>HoxB6</b>	<b>UN</b>	<b>UN</b>	<b>UN</b>	<b>UN</b>	<b>UN</b>	<b>UN</b>	<b>1.01</b> (1.13–0.89)	<b>0.377</b> (0.826–0.172)	<b>0.878</b> (0.957–0.806)
<b>HoxB7</b>	<b>UN</b>	<b>UN</b>	<b>UN</b>	<b>UN</b>	<b>UN</b>	<b>UN</b>	<b>1.02</b> (1.26–0.79)	<b>1.33</b> (1.53–1.13)	<b>1.319</b> (1.504–1.157)
<b>HoxB8</b>	<b>UN</b>	<b>UN</b>	<b>UN</b>	<b>UN</b>	<b>UN</b>	<b>UN</b>	<b>UN</b>	<b>UN</b>	<b>UN</b>
<b>HoxB9</b>	<b>UN</b>	<b>UN</b>	<b>UN</b>	<b>UN</b>	<b>UN</b>	<b>UN</b>	<b>UN</b>	<b>UN</b>	<b>UN</b>

The hours (h) refer to the NT2-D1 cultures' time of exposure to 1  $\mu$ M of retinoic acid (RA, added at the 0h time point). When present, cytochalasin D (CytD, 100 nM) or latrunculin A (LatA, 50 nM) were added at different time points depending on the treatment, i.e., t = 0h is the 0h time point for the 16-h RA treatment (16h+CytD t = 0h), t = 24h is the 24h time point for the 48-h RA treatment (48h+CytD t = 24h), and t = 48h is the 48h time point for the 72-h RA treatment (72h+CytD t = 48h). The data are expressed as the mean expression after RA induction set equal to 1.0; the values below represent the confidence interval at 95%. The data represent the average of triplicate RT-q-PCR experiment from three biological independent experiments. UN: undetermined values by RT-q-PCR. Control transcripts' levels (cultures treated with DMSO) are equal to zero (not shown).

in the transcription/splicing of the *HoxB* gene cluster (for quantification of co-localization see Fig. S1B).

#### Nuclear actin polymerization activates *HoxB* cluster transcription

We hypothesized that *HoxB* gene expression depends on the polymerization of nuclear actin. To investigate if actin polymerization is required for the activation of the *HoxB* cluster, we analyzed the collinear transcription of the cluster in the presence of actin polymerization inhibitors (toxins) Cytochalasin D (CytD) and Latrunculin A (LatA). LatA inhibits actin polymerization not by capping the faster growing ends of filaments, as CytD does, but by delaying general polymerization through the recruitment of actin monomers.<sup>28</sup>

Table 1, which was published in part in our previous work (Ferrai et al., 2009) is hereby enhanced, re-analyzed and reviewed. In order to do this, the data regarding CytD action on *HoxB* gene collinear expression have been contrasted to the data regarding LatA action on the same process. Here, the levels of RA-induced transcripts in NT2-D1 cells treated with CytD and LatA are shown. The first transcripts of the cluster, namely *HoxB1* and *HoxB2* are detected after 16 h of RA treatment. Therefore, CytD or LatA were added at the time of induction lasting 16h, to overlap with the RA treatment (16h+CytD t = 0h or 16h+Lat A t = 0h, Table 1). In the presence of CytD, *HoxB1* and *HoxB2* transcription is not induced, which suggests that their expression was blocked by the toxin. On the other hand, LatA does not affect RA induction of the *HoxB1* and *HoxB2* genes (16h+LatA t = 0h, Table 1). To determine that the effect was not a non-specific effect on transcription, we

analyzed the expression of an RA-inducible gene, *Pbx1*, and two RA-non-inducible ones, *Bike* and *Eps8*. The expression of these genes that were not affected by toxins is shown in Table S1. The next collinear gene in the cluster, *HoxB3*, is expressed 48h after RA induction of the cells. *HoxB3* expression was blocked when CytD was added to cultures 24h after the initiation of the RA treatment (48+CytD t = 24h, see Table 1). Noteworthy, addition of CytD 24h after initiation of the 48 h-RA treatment, however, does not affect the levels of *HoxB1* and *HoxB2* transcripts, which are used as internal controls, indicating that CytD do not affect the whole cluster (Table 1). The subsequent collinear genes, *HoxB4* and *HoxB5*, also remained unchanged. When CytD was added at 48h within a 72 h-RA treatment, induction of *HoxB6* gene transcription was also blocked (72h+CytD t = 48h, Table 1), while *HoxB1*, *HoxB2*, *HoxB3*, *HoxB4* and *HoxB5*, and its subsequent collinear *HoxB7*, did not change the transcription level. Taken together, the results strongly suggest that CytD inhibits the initial activation of *HoxB* gene transcription. The addition of LatA to the cell culture in the same conditions as with CytD results in diminished expression of the *HoxB2*, *HoxB3*, *HoxB4* and *HoxB5* transcripts, although in a less dramatic level as with CytD (Table 1). This suggests that LatA might slow down *HoxB* cluster transcription. However, it does not cause any decrease of the control genes transcript expression level (Table S1). Taking into account that CytD inhibits nuclear actin polymerization by capping the plus ends, we hypothesized that the faster growing ends of the actin filaments are involved in the transcriptional activation of the *HoxB* cluster. To rule out that the toxins affect the process of transcription

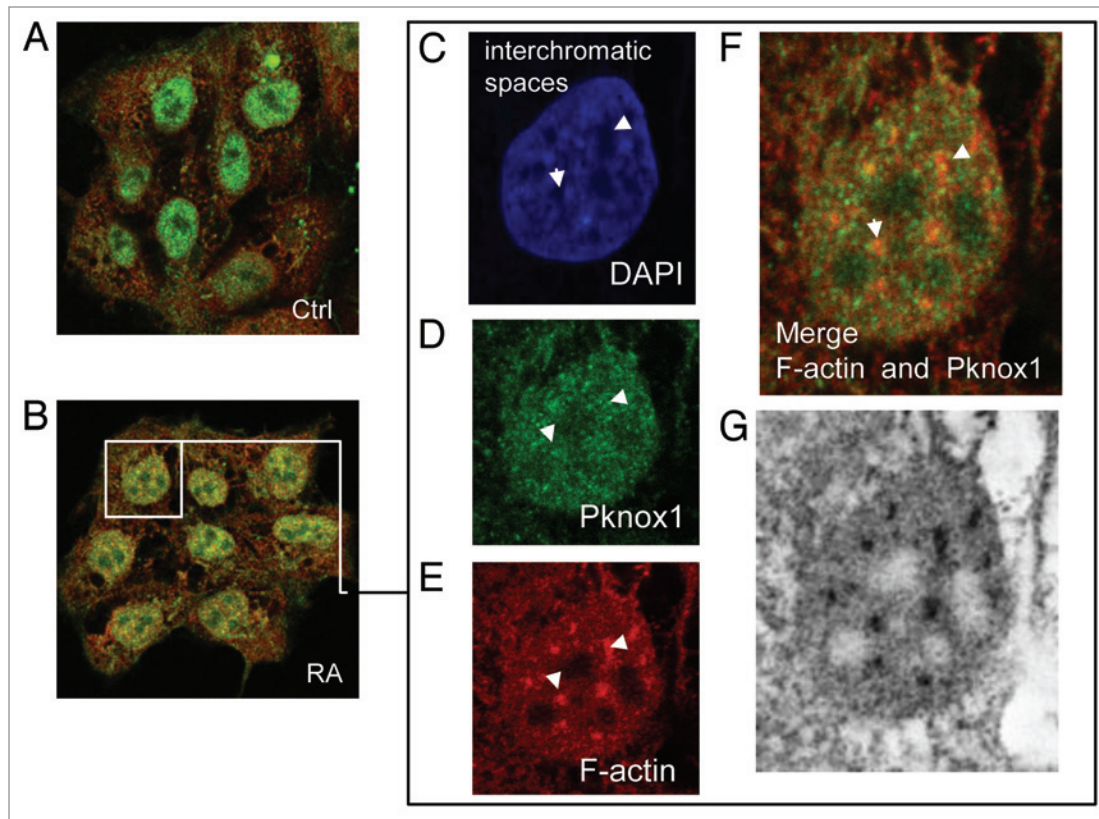


**Figure 7.** Retinoic acid induces co-localization between F-actin and Pknox1 in the nucleus of NT2-D1 cells. Control NT2-D1 cells (Ctrl) and retinoic-acid treated cells (RA) are shown as immunofluorescence merges (A and B). C to F show a nucleus of RA-treated cells at higher magnification (63X magnification plus an 8X confocal microscope software zoom). In panel C, the RA-treated NT2-D1 nucleus is shown in blue (DAPI staining). Pknox1 is shown in green (D) and polymeric actin, in red (E). Merges between polymeric actin and Pknox1 are shown (F). The merge between polymeric actin (red) and Pknox1 (green) is shown in panel F. As it can be observed these proteins co-localize particularly in the interchromatic spaces (C, arrow heads; F, yellow). Co-localization between F-actin and Pknox1 shows a speckled pattern (G).

even when initiated, we studied the initial activation of *HoxB1* and *HoxB2* transcription shortly after RA induction, NT2-D1 cells were treated with RA for 3 h in the absence of toxins and then, at time point 3h, CytD or LatA were added for 16 h in the presence of RA (Table 2, 19h+CytD t = 3h or 19h+LatA t = 3h). The rationale of the experiment is that the cells are free of actin polymerization inhibitors during the initial activation of *HoxB1* and *HoxB2* transcription. Table 2 shows that once transcription is initiated and a steady-state is reached, the level of both transcripts remains unaffected. These results indicate that nuclear actin polymerization is critical for gene expression during the early transcriptional activation events (for details about treatments see Fig. S2).

#### A model for actin-dependent collinearity of *HoxB* gene expression by nuclear speckles

Our results indicate that CytD only inhibits *Hox* gene expression at the early steps of transcriptional activation. This suggests a narrow time frame for CytD action at the beginning of the transcription of *HoxB* genes, which is supported by the lack of inhibition by CytD when transcription has already been induced by RA and reaches a steady-state (Fig. 8A). Thus, we can hypothesize that the faster growing ends of actin filaments play a role in the early activation of *HoxB* transcription.

Splicing occurs in nuclear speckles, in the close vicinity of genes and is frequently co-transcriptional.<sup>43</sup> This way, we propose that additional transcription/splicing factors, such as p54<sup>nrb</sup>, which binds DNA and, in turn, N-WASP, might connect gene regulatory elements to nuclear speckles by means of nuclear polymeric actin. This would explain the control of the *Hox* gene expression from the beginning, through the organized movement of the cluster in the interphase nucleus. The motor mechanism of the *HoxB* cluster movement, and of its related proteins (transcription/splicing machinery), might occur at the early steps of transcription. Thus, the collinearity of the expression and the timing of transcriptional activation of the cluster might depend on the formation of nuclear polymeric actin, which could polymerize into nuclear speckles. These compartments might coordinate the chromatin movement during the co-transcriptional splicing process. They could act as “roundabouts” connecting the rails to direct the movement of the gene cluster within the nucleus for the transcription/splicing process and mRNA export. This implies that chromatin should be moved by the actin filaments through the nuclear speckles machinery and that polymerization of actin into nuclear speckles could be involved in the initiation of transcription once a gene gets in there. However, we cannot determine yet which is the initial molecular event (promoter activation,

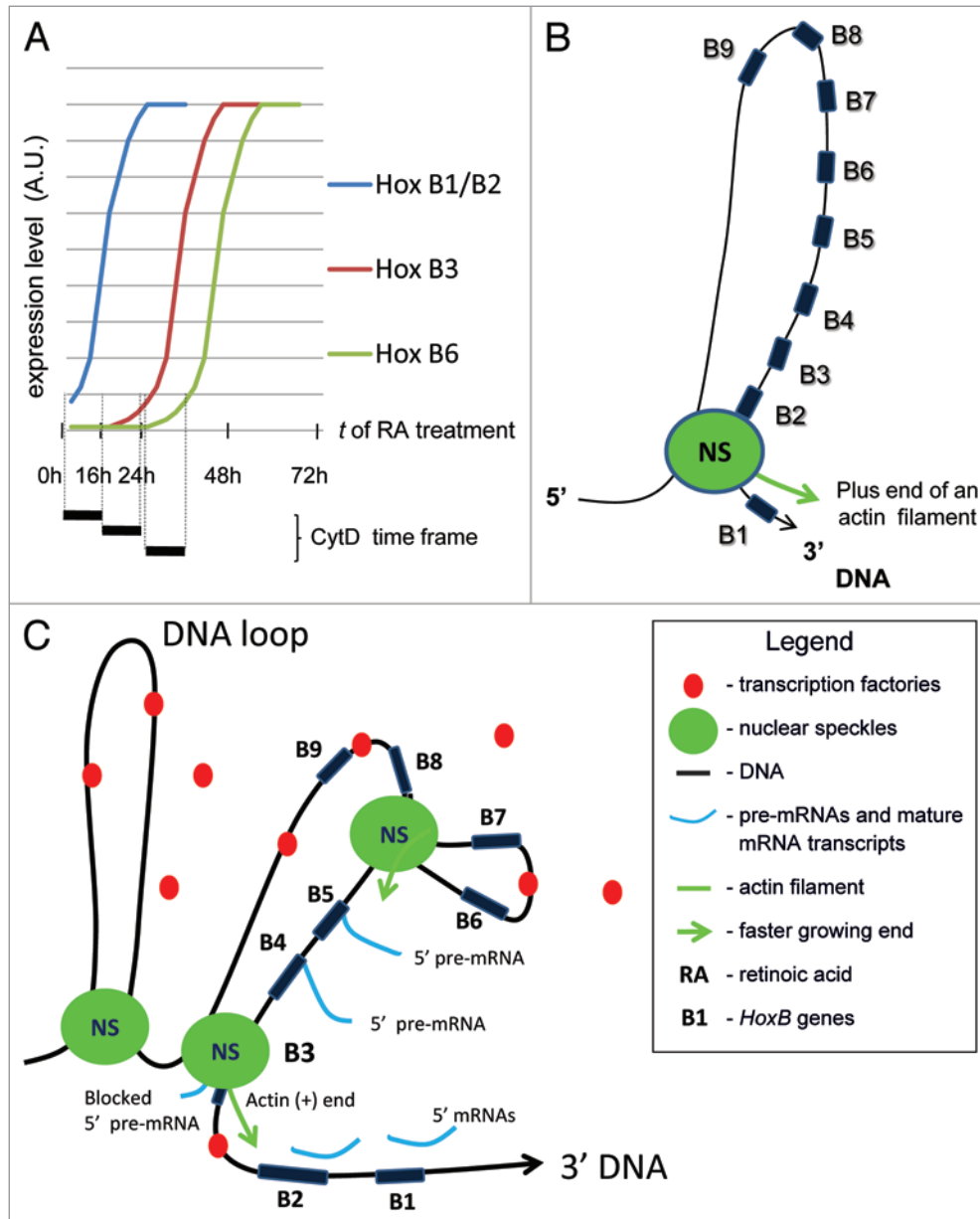


**Figure 8.** (A) Schematic curves of *HoxB1/B2*, *HoxB3* and *HoxB6* expression. When indicated, cytochalasin D (CytD) was added to the medium with retinoic acid (RA) for 16 or 24 h before quantification. Observe that, at hours 16, 48 and 72, *HoxB1/B2*, *HoxB3* and *HoxB6* transcripts, respectively, reach linear expression to the steady-state. Time frames for CytD-action at the beginning of the expression are shown below (black bars). Time (*t*) is expressed in hours (h). Transcript levels are expressed as arbitrary units (A.U.). (B) Model for the role of nuclear actin polymerization in the expression of *HoxB* genes. This model is the simplest interpretation of the data presented in Table 1. The lack of inhibition by CytD when the level of transcripts is induced by RA (before reaching the steady-state) implies collinearity and dependence on nuclear actin polymerization in the expression of the *HoxB* cluster. CytD acts in a narrow time frame at the moment of the initial activation of transcription, and nuclear actin polymerization could be the mechanism for the transport of chromatin to a site where RNAP II and other factors are placed (transcription factories and/or nuclear speckles). (C) Model for the role of nuclear actin polymerization in the coordinated expression of *HoxB* genes by means of nuclear speckles. CytD blocks actin polymerization from the faster growing end of the actin filaments. Once transcription is initiated, CytD has no action over the expression of the genes. It is not possible to rule out that, once in the speckle, the start-up of the cluster transcription could initiate and that nuclear actin polymerization could continue to move chromatin through the nuclear compartments. RNAP II could be fixed at nuclear speckles where nuclear actin aggregates are placed and might be released from chromatin prior to the completion of the pre-mRNAs processing while the pre-mRNAs are still tethered to chromatin near the gene end. This could be the reason by which only the gene that is related to the actin machinery is sensitive to CytD, while the upstream and downstream genes in the cluster do not, being expressed in self-assembled transcriptional machineries.

**Table 2.** Cytochalasin D and Latrunculin A effect on the RA-induced Hox gene initial activation of transcription

GENES	C	RA		
		Toxin free	19h + CytD t = 3h	19h + LatA t = 3h
<b>HoxB1</b>	<b>0.179</b> (0.203–0.158)	<b>1</b> (1.164–0.859)	<b>1.288</b> (1.518- 1.092)	<b>1.337</b> (1.525- 1.173)
<b>HoxB2</b>	<b>0.05</b> (0.054–0.046)	<b>1</b> (1.255–0.797)	<b>1.211</b> (1.401- 1.047)	<b>1.216</b> (1.378- 1.073)
<b>HoxB3</b>	<b>UN</b>	<b>UN</b>	<b>UN</b>	<b>UN</b>
<b>Bike</b>	<b>0.992</b> (1.105–0.891)	<b>1</b> (0.883- 1.132)	<b>1.382</b> (1.648–1.159)	<b>1.089</b> (1.262–0.939)

The hours (h) refer to the NT2-D1 cultures' time of exposure to 1  $\mu$ M retinoic acid (RA, added at the 0h time point). When present, cytochalasin D (CytD, 100 nM) or latrunculin A (LatA, 50 nM) were added at the 3h time point (t = 3h) for the 19-h RA treatment (19h+CytD t = 3h or 19h+LatA t = 3h). Bike is a control gene. The data are shown as the mean expression after RA induction set equal to 1.0; the values below represent the confidence interval at 95%. Toxin Free indicates the transcript level values of the RA-treated cultures free of toxins or actin-interfering drugs; these values were set to 1.0. The data represent the average of triplicate RT-q-PCR experiment from two biological independent experiments. UN: undetermined values by RT-q-PCR.

polymerase binding, TAF interactions), which will require further investigations. The model in **Figure 8B** is the simplest interpretation of our data, according to the concepts that 1) *HoxB* cluster moves in order to be transcribed upon RA induction and, most importantly, 2) the faster growing ends of nuclear actin filaments are involved in the initial activation of the *HoxB* transcription process. Nevertheless, we cannot rule out that nuclear actin polymerization may continue to move chromatin through either the speckles or other transcriptional active compartments and that the CytD inhibition of a gene in the cluster does affect the upstream and downstream transcriptional unit expression that might take place at the speckle (i.e., *HoxB1/B2* and *HoxB4* with respect to *HoxB3*). In this sense, RNAP II should be fixed at nuclear speckles where nuclear actin aggregates are placed. This means that only the gene that is related to the actin machinery is sensitive to CytD, while upstream and downstream genes in the cluster might be expressed in self-assembled transcriptional machineries as transcription factories, where RNA polymerase molecules are in motion.

Most of the pre-mRNA processing events, such as splicing, editing, 3' processing, and polyadenylation of mRNAs, occur co-transcriptionally, while the RNA polymerase II is engaged in transcriptional elongation. Nevertheless, recent evidence has shown that retention of polyadenylated mRNAs was detected at the transcription site after transcription termination. This implies that the polymerase is released from chromatin prior to the completion of splicing, and the pre-mRNA is

post-transcriptionally processed while still tethered to chromatin near the gene end.<sup>44</sup> According to this lighting, downstream pre-mRNAs could be detected because they could still be tethered to chromatin by its 3' ends (behind the nuclear speckle). This will lead to a more complex model that—despite being a challenging framework hypothesis—will still require experimental evidence (**Fig. 8C**).

In summary, our model suggests that nuclear actin polymerization is a critical process for the coordination of the expression of the *HoxB* gene cluster, and contributes—as an additional driving force, together with other motor proteins—to move chromatin into the transcription/splicing machinery for the organized collinear expression of the cluster.

#### Acknowledgments

This work was supported by CONICET (PIP0247/2011 to GNO), ANPCyT (PICT1528/2008 to GNO and PICT 1237/2008 to RRP) and the Max Planck External Partner Laboratory Program to RRP. GNO and RRP are investigators of CONICET (Argentina).

#### Disclosure of Potential Conflicts of Interest

No potential conflicts of interest were disclosed.

#### Supplemental Materials

Supplemental materials may be downloaded here: [www.landesbioscience.com/journals/transcription/article/27672/](http://www.landesbioscience.com/journals/transcription/article/27672/)

#### References

- Caron H, van Schaik B, van der Mee M, Baas F, Riggins G, van Sluis P, Hermus MC, van Asperen R, Boon K, Voûte PA, et al. The human transcriptome map: clustering of highly expressed genes in chromosomal domains. *Science* 2001; 291:1289-92; PMID:11181992; <http://dx.doi.org/10.1126/science.1056794>
- Kosak ST, Groudine M. Gene order and dynamic domains. *Science* 2004; 306:644-7; PMID:15499009; <http://dx.doi.org/10.1126/science.1103864>
- Jackson DA. The amazing complexity of transcription factories. *Brief Funct Genomic Proteomic* 2005; 4:143-57; PMID:16102270; <http://dx.doi.org/10.1093/bfgp/4.2.143>
- Chambeyron S, Bickmore WA. Chromatin decondensation and nuclear reorganization of the HoxB locus upon induction of transcription. *Genes Dev* 2004; 18:1119-30; PMID:15155579; <http://dx.doi.org/10.1101/gad.292104>
- Sutherland H, Bickmore WA. Transcription factories: gene expression in unions? *Nat Rev Genet* 2009; 10:457-66; PMID:19506577; <http://dx.doi.org/10.1038/nrg2592>
- Papantoni A, Larkin JD, Wada Y, Ohta Y, Ihara S, Kodama T, Cook PR. Active RNA polymerases: mobile or immobile molecular machines? *PLoS Biol* 2010; 8:e1000419; PMID:20644712; <http://dx.doi.org/10.1371/journal.pbio.1000419>
- Cisse II, Izeddin I, Causse SZ, Boudarene L, Senecal A, Muresan L, Dugast-Darzacq C, Hajj B, Dahan M, Darzacq X. Real-time dynamics of RNA polymerase II clustering in live human cells. *Science* 2013; 341:664-7; PMID:23828889; <http://dx.doi.org/10.1126/science.1239053>
- Yao J, Ardehali MB, Fecko CJ, Webb WW, Lis JT. Intranuclear distribution and local dynamics of RNA polymerase II during transcription activation. *Mol Cell* 2007; 28:978-90; PMID:18158896; <http://dx.doi.org/10.1016/j.molcel.2007.10.017>
- Shopland LS, Johnson CV, Byron M, McNeil J, Lawrence JB. Clustering of multiple specific genes and gene-rich R-bands around SC-35 domains: evidence for local euchromatic neighborhoods. *J Cell Biol* 2003; 162:981-90; PMID:12975345; <http://dx.doi.org/10.1083/jcb.200303131>

10. Brown JM, Green J, das Neves RP, Wallace HA, Smith AJ, Hughes J, Gray N, Taylor S, Wood WG, Higgs DR, et al. Association between active genes occurs at nuclear speckles and is modulated by chromatin environment. *J Cell Biol* 2008; 182:1083-97; PMID:18809724; <http://dx.doi.org/10.1083/jcb.200803174>
11. Hu Y, Plutz M, Belmont AS. Hsp70 gene association with nuclear speckles is Hsp70 promoter specific. *J Cell Biol* 2010; 191:711-9; PMID:21059845; <http://dx.doi.org/10.1083/jcb.201004041>
12. Simeone A, Acampora D, Arcioni L, Andrews PW, Boncinelli E, Mavilio F. Sequential activation of HOX2 homeobox genes by retinoic acid in human embryonal carcinoma cells. *Nature* 1990; 346:763-6; PMID:1975088; <http://dx.doi.org/10.1038/346763a0>
13. Krumlauf R. Hox genes in vertebrate development. *Cell* 1994; 78:191-201; PMID:7913880; [http://dx.doi.org/10.1016/0092-8674\(94\)90290-9](http://dx.doi.org/10.1016/0092-8674(94)90290-9)
14. Morey C, Kress C, Bickmore WA. Lack of bystander activation shows that localization exterior to chromosome territories is not sufficient to up-regulate gene expression. *Genome Res* 2009; 19:1184-94; PMID:19389823; <http://dx.doi.org/10.1101/gr.089045.108>
15. Berthelsen J, Zappavigna V, Ferretti E, Mavilio F, Blasi F. The novel homeoprotein Prep1 modulates Pbx-Hox protein cooperativity. *EMBO J* 1998; 17:1434-45; PMID:9482740; <http://dx.doi.org/10.1093/emboj/17.5.1434>
16. Ferretti E, Marshall H, Pöpperl H, Maconochie M, Krumlauf R, Blasi F. Segmental expression of Hoxb2 in r4 requires two separate sites that integrate cooperative interactions between Prep1, Pbx and Hox proteins. *Development* 2000; 127:155-66; PMID:10654609
17. Ferretti E, Cambrono F, Tümpel S, Longobardi E, Wiedemann LM, Blasi F, Krumlauf R. Hoxb1 enhancer and control of rhombomere 4 expression: complex interplay between PREP1-PBX1-HOXB1 binding sites. *Mol Cell Biol* 2005; 25:8541-52; PMID:16166636; <http://dx.doi.org/10.1128/MCB.25.19.8541-8552.2005>
18. Manzanera M, Bel-Vialar S, Ariza-McNaughton L, Ferretti E, Marshall H, Maconochie MM, Blasi F, Krumlauf R. Independent regulation of initiation and maintenance phases of Hoxa3 expression in the vertebrate hindbrain involve auto- and cross-regulatory mechanisms. *Development* 2001; 128:3595-607; PMID:11566863
19. Jacobs Y, Schnabel CA, Cleary ML. Trimeric association of Hox and TALE homeodomain proteins mediates Hoxb2 hindbrain enhancer activity. *Mol Cell Biol* 1999; 19:5134-42; PMID:10373562
20. Díaz VM, Bachi A, Blasi F. Purification of the Prep1 interactome identifies novel pathways regulated by Prep1. *Proteomics* 2007; 7:2617-23; PMID:17623278; <http://dx.doi.org/10.1002/pmic.200700197>
21. Olave IA, Reck-Peterson SL, Crabtree GR. Nuclear actin and actin-related proteins in chromatin remodeling. *Annu Rev Biochem* 2002; 71:755-81; PMID:12045110; <http://dx.doi.org/10.1146/annurev.biochem.71.110601.135507>
22. Philimonenko VV, Zhao J, Iben S, Dingová H, Kyselá K, Kahle M, Zentgraf H, Hofmann WA, de Lanerolle P, Hozák P, et al. Nuclear actin and myosin I are required for RNA polymerase I transcription. *Nat Cell Biol* 2004; 6:1165-72; PMID:15558034; <http://dx.doi.org/10.1038/ncb1190>
23. Hofmann WA, Stojiljkovic L, Fuchsova B, Vargas GM, Mavrommatis E, Philimonenko V, Kyselá K, Goodrich JA, Lessard JL, Hope TJ, et al. Actin is part of pre-initiation complexes and is necessary for transcription by RNA polymerase II. *Nat Cell Biol* 2004; 6:1094-101; PMID:15502823; <http://dx.doi.org/10.1038/ncb1182>
24. Hu P, Wu S, Hernandez N. A role for  $\beta$ -actin in RNA polymerase III transcription. *Genes Dev* 2004; 18:3010-5; PMID:15574586; <http://dx.doi.org/10.1101/gad.1250804>
25. Wu X, Yoo Y, Okuhama NN, Tucker PW, Liu G, Guan JL. Regulation of RNA-polymerase-II-dependent transcription by N-WASP and its nuclear-binding partners. *Nat Cell Biol* 2006; 8:756-63; PMID:16767080; <http://dx.doi.org/10.1038/ncb1433>
26. Yoo Y, Wu X, Guan JL. A novel role of the actin-nucleating Arp2/3 complex in the regulation of RNA polymerase II-dependent transcription. *J Biol Chem* 2007; 282:7616-23; PMID:17220302; <http://dx.doi.org/10.1074/jbc.M607596200>
27. McDonald D, Carrero G, Andrin C, de Vries G, Hendzel MJ. Nucleoplasmic beta-actin exists in a dynamic equilibrium between low-mobility polymeric species and rapidly diffusing populations. *J Cell Biol* 2006; 172:541-52; PMID:16476775; <http://dx.doi.org/10.1083/jcb.200507101>
28. Cooper JA. Effects of cytochalasin and phalloidin on actin. *J Cell Biol* 1987; 105:1473-8; PMID:3312229; <http://dx.doi.org/10.1083/jcb.105.4.1473>
29. Ferrai C, Naum-Ongania G, Longobardi E, Palazzolo M, Disanza A, Diaz VM, Crippa MP, Scita G, Blasi F. Induction of HoxB transcription by retinoic acid requires actin polymerization. *Mol Biol Cell* 2009; 20:3543-51; PMID:19477923; <http://dx.doi.org/10.1091/mbc.E09-02-0114>
30. Spinella MJ, Freemantle SJ, Sekula D, Chang JH, Christie AJ, Dmitrovsky E. Retinoic acid promotes ubiquitination and proteolysis of cyclin D1 during induced tumor cell differentiation. *J Biol Chem* 1999; 274:22013-8; PMID:10419526; <http://dx.doi.org/10.1074/jbc.274.31.22013>
31. O'Neill C, Jordan P, Ireland G. Evidence for two distinct mechanisms of anchorage stimulation in freshly explanted and 3T3 Swiss mouse fibroblasts. *Cell* 1986; 44:489-96; PMID:3943134; [http://dx.doi.org/10.1016/0092-8674\(86\)90470-8](http://dx.doi.org/10.1016/0092-8674(86)90470-8)
32. Dignam JD, Martin PL, Shastri BS, Roeder RG. Eukaryotic gene transcription with purified components. *Methods Enzymol* 1983; 101:582-98; PMID:6888276; [http://dx.doi.org/10.1016/0076-6879\(83\)01039-3](http://dx.doi.org/10.1016/0076-6879(83)01039-3)
33. Andrews PW. Retinoic acid induces neuronal differentiation of a cloned human embryonal carcinoma cell line in vitro. *Dev Biol* 1984; 103:285-93; PMID:6144603; [http://dx.doi.org/10.1016/0012-1606\(84\)90316-6](http://dx.doi.org/10.1016/0012-1606(84)90316-6)
34. Fisher D, Méchali M. Vertebrate HoxB gene expression requires DNA replication. *EMBO J* 2003; 22:3737-48; PMID:12853488; <http://dx.doi.org/10.1093/emboj/edg352>
35. Masuda S, Das R, Cheng H, Hurt E, Dorman N, Reed R. Recruitment of the human TREX complex to mRNA during splicing. *Genes Dev* 2005; 19:1512-7; PMID:15998806; <http://dx.doi.org/10.1101/gad.1302205>
36. Durfee T, Mancini MA, Jones D, Elledge SJ, Lee WH. The amino-terminal region of the retinoblastoma gene product binds a novel nuclear matrix protein that co-localizes to centers for RNA processing. *J Cell Biol* 1994; 127:609-22; PMID:7525595; <http://dx.doi.org/10.1083/jcb.127.3.609>
37. Li Y, Wang X, Zhang X, Goodrich DW. Human hHpr1/p84/Thoc1 regulates transcriptional elongation and physically links RNA polymerase II and RNA processing factors. *Mol Cell Biol* 2005; 25:4023-33; PMID:15870275; <http://dx.doi.org/10.1128/MCB.25.10.4023-4033.2005>
38. Palazzolo M, Berthelsen J, De Cesare D, Blasi F. Oct-1 specifically binds the UEF4 site of the human AP1-regulated urokinase enhancer. *Eur J Biochem* 2000; 267:5427-37; PMID:10951201; <http://dx.doi.org/10.1046/j.1432-1327.2000.01604.x>
39. Eraly SA, Nelson SB, Huang KM, Mellon PL. Oct-1 binds promoter elements required for transcription of the GnRH gene. *Mol Endocrinol* 1998; 12:469-81; PMID:9544983; <http://dx.doi.org/10.1210/me.12.4.469>
40. Shav-Tal Y, Zipori D. PSF and p54(nrb)/NonO-multi-functional nuclear proteins. *FEBS Lett* 2002; 531:109-14; PMID:12417296; [http://dx.doi.org/10.1016/S0014-5793\(02\)03447-6](http://dx.doi.org/10.1016/S0014-5793(02)03447-6)
41. Kameoka S, Duque P, Konarska MM. p54(nrb) associates with the 5' splice site within large transcription/splicing complexes. *EMBO J* 2004; 23:1782-91; PMID:15057275; <http://dx.doi.org/10.1038/sj.emboj.7600187>
42. Rosonina E, Ip JY, Calarco JA, Bakowski MA, Emili A, McCracken S, Tucker P, Ingles CJ, Blencowe BJ. Role for PSF in mediating transcriptional activator-dependent stimulation of pre-mRNA processing in vivo. *Mol Cell Biol* 2005; 25:6734-46; PMID:16024807; <http://dx.doi.org/10.1128/MCB.25.15.6734-6746.2005>
43. Kornbliht AR, de la Mata M, Fededa JP, Muñoz MJ, Nogues G. Multiple links between transcription and splicing. *RNA* 2004; 10:1489-98; PMID:15383674; <http://dx.doi.org/10.1261/rna.7100104>
44. Brody Y, Neufeld N, Bieberstein N, Causse SZ, Böhnlein EM, Neugebauer KM, Darzacq X, Shav-Tal Y. The in vivo kinetics of RNA polymerase II elongation during co-transcriptional splicing. *PLoS Biol* 2011; 9:e1000573; <http://dx.doi.org/10.1371/journal.pbio.1000573>; PMID:21264352